eigenvalues are all real and positive; for an isotropic parabolic band the eigenfunctions of K are Sonine polynomials and the eigenvalues are $n\gamma_r/m^*$, with γ_r given by Eq. (3.13).

In the limit $\omega \to \infty$,

$$\sigma^{(N)} \to -i(e^2/\omega)K_{00}. \tag{A6}$$

The meaning of K_{00} can be found by considering the dc conductivity under a scattering mechanism represented by a constant relaxation time. Under these conditions, from Eq. (3.22),

$$\sigma_0 = e^2\tau K_{00}. \tag{A7}$$

Hence

$$K_{00} = n/m^*, \tag{A8}$$

where m^* is the effective mass determining the conductivity. A general expression for m^* is obtained by comparing Eqs. (A8) and (A3).

The poles of $\sigma^{(N)}$, regarded as a function of the complex variable ω, are the zeros of the determinant $|L+i\omega K|$, as all the matrix elements of L and K are finite. Consider the equation

$$|L-\lambda K| = 0. \tag{A9}$$

Because L and K are Hermitian and positive definite it follows that all the roots λ are real and positive. The poles of Eq. (A5) are then given by Eq. (A9) with $\lambda = -i\omega$. Hence $\sigma^{(N)}$ is analytic in the lower half of the ω plane, like the exact solution σ. By integration round an infinite semicircular contour closed round the lower half plane, using Eqs. (A6) and (A8), the sum rule (2.13) is obtained.

PHYSICAL REVIEW VOLUME 140, NUMBER 1A 4 OCTOBER 1965

Intrinsic and Extrinsic Recombination Radiation from Natural and Synthetic Aluminum-Doped Diamond

P. J. Dean, E. C. Lightowlers, and D. R. Wight
Wheatstone Laboratory, King's College, London, England
(Received 3 May 1965)

The edge-recombination-radiation spectrum from natural semiconducting diamond has been re-examined and compared with spectra obtained for the first time from aluminum and nominally boron-doped General Electric synthetic diamond. The intrinsic components are due to the phonon-assisted decay of free indirect excitons of internal binding energy ~0.08 eV. Comparison of the phonon energies with recently obtained dispersion curves for the fundamental lattice vibrations shows that the conduction-band minima are located at points $\frac{3}{4}$ of the way from the center to the ⟨100⟩ boundaries of the reduced zone. Substructure has been observed in the intrinsic components due to the ~7-meV spin-orbit splitting in the valence-band energy states at the zone center. The major extrinsic components are due to the zero-phonon and phonon-assisted decay of excitons bound to a characteristic acceptor center of semiconducting diamond (E_A=0.36 eV). The bound excitons have a thermal and optical ionization energy of ~50 meV. These extrinsic components exhibit enhanced spin-orbit splitting (~12 meV). Radiation due to the zero-phonon and phonon-assisted recombination of free electrons at the neutral acceptor center has been detected. Infrared absorption measurements, neutron-activation analysis, and electrical-transport (Hall-effect) measurements have also been made. Intercomparison of these results and the edge-emission data shows that the acceptor center is due to isolated substitutional aluminum impurities. These acceptor centers are considerably more abundant in the synthetic diamonds, but the degree of compensation is generally much higher than in the available natural semiconducting specimens. Nitrogen donors with very deep energy levels apparently play a major role in the compensation.

I. INTRODUCTION

RECOMBINATION radiation of quantum energy close to the indirect energy gap, E_g=5.5 eV, of natural semiconducting diamond (type IIb)[1] has already been discussed.[2] Comparisons of results obtained from the latest edge-emission spectra with the lattice-vibrational dispersion curves recently measured by the inelastic scattering of slow neutrons[3] shows that the previous interpretation must be revised. The present paper shows that a very satisfactory description of the indirect gap transitions is obtained using the new lattice-dispersion data. The diamond spectra prove to be remarkably similar to the well-known recombination-radiation spectra of silicon,[4] the main differences arising from the very small spin-orbit valence-band splitting and the more compact wave functions for the electronic complexes in diamond.

In the previous work, edge emission from insulating General Electric synthetic diamonds was looked for

[1] C. D. Clark, R. W. Ditchburn, and H. B. Dyer, Proc. Roy. Soc. (London) **A234**, 363 (1956). The classification of natural diamonds by absorption spectra is discussed in this reference.
[2] P. J. Dean and I. H. Jones, Phys. Rev. **133**, A1698 (1964).
[3] J. L. Warren, R. G. Wenzel, and J. L. Yarnell, Phys. Rev. (to be published).
[4] J. R. Haynes, M. Lax, and W. F. Flood, J. Phys. Chem. Solids **8**, 392 (1959).

without success. Since then, useful spectra have been obtained from doped synthetic (semiconducting) specimens. The principal components in the spectra from these synthetic diamonds are very similar to those previously described from type-IIb natural diamonds.

Improvements in experimental technique have facilitated more sensitive spectral investigations, and several new intrinsic and extrinsic emission components have been discovered. The present discussion of the extrinsic components is restricted to those which can be associated with transitions involving the acceptor center which is characteristic of natural type-IIb diamond. Optical, electrical (Hall-effect), and neutron-activation-analysis experiments provide strong evidence for the identification of this prevalent acceptor center with dispersed substitutional aluminum.

II. EXPERIMENTAL

A. Optical Emission

The recombination radiation was excited by an electron beam. Typically a 20-μA beam of 60-keV electrons was focused onto a region of the specimen between 0.1 and 0.5 mm in diameter. The previously used apparatus[2] was simplified and largely rebuilt using stainless steel so that a working vacuum of $\sim 10^{-5}$ mm Hg could be obtained near the electron gun, thus reducing the amount of ion bombardment of the specimen surface to a tolerable level. The optical system was simplified and a different recording monochromator with improved resolution was developed. Spectra have been obtained of the weak edge emission from many specimens with a signal-to-noise ratio of $>100:1$ at the peak of the principal components, using a Rayleigh resolving power of ~ 2000 (3-meV spectral slitwidth).

The specimens are mounted in indium pressed into a copper boat which forms part of the cold finger of a stainless-steel Dewar. The axis of the Dewar and the specimen surface are usually set at 45° to the vertical electron beam and the emission is viewed in the horizontal plane. Close attention was paid to the thermal contact between the specimen and the Dewar since $\gtrsim 1$ W of electrical power was dissipated within a volume of $\sim 10^{-6}$ cm^3 in the specimen. This corresponds to a generation rate of free carriers of $\sim 10^{23}$ cm^{-3}, since the mean energy required to form one electron-hole pair is ~ 20 eV.[5] Some of the synthetic specimens have only $\sim 10^{-5}$ cm^{-3} total volume.

The temperature of specimens under irradiation was estimated from tests made with a 1.5-mm-diam type-IIa specimen which has a 0.35-mm hole bored into its surface. A thermocouple junction was packed into the hole with indium. The difference between the specimen and Dewar temperature was measured as a function of the intensity of the 60-keV electron beam focused onto the specimen close to the thermocouple junction. For a typical beam current ($\sim 20\,\mu$A) this difference was +15°C with the Dewar at 80°K. Calculations show that the temperature difference between adjacent interior portions of the diamonds should be negligible compared with this indicated difference, since the thermal conductivity of these relatively perfect specimens is ~ 100 W cm^{-1} °K^{-1} at 100°K.

Edge emission can only be obtained from relatively perfect diamonds. Nitrogen donors, both in associated (type-I[6]) and dispersed[7] configurations, together with the defects introduced by irradiation damage, efficiently inhibit the edge radiation.

B. Electrical-Transport Measurements

Measurements of the Hall effect and conductivity were made between ~ 200°K and ~ 1000°K in order to obtain essentially complete thermal dissociation of the acceptor centers of type-IIb natural semiconducting diamond ($E_A \sim 0.36$ eV). A specially designed furnace and cryostat was used for measurements, respectively, above and below 300°K.[8] Conventional techniques were used to prepare the contacts between tungsten wires and the rectangular-parallelepiped specimens. Considerable efforts were made to ensure that the side contacts (spots of Degussa No. 200 silver paint ~ 0.1-mm diam) were as small as possible compared with the specimen length (2 to 3 mm). The crystals were pressed by the contact wires onto a fused silica plate and the wires were attached to the plate with Sauereisen ceramic cement.

The plate was bolted to a copper heater block with large thermal capacity, so that measurements could be made without the use of a servo control system to stabilize the specimen temperature. With care, the four sets of Hall and conductivity potentials for the possible combinations of the direction of magnetic field and transverse current flow, together with the magnetic field and the temperature, could be recorded within a 1°C temperature change of the furnace. Care was taken in the mounting and during the measurements to minimize the effect of rectification at the current contacts, of the magnitude of the misalignment voltage at the Hall contacts and of the thermoelectric potentials. These effects are very troublesome in electrical measurements on diamond because of the inconveniently large temperature range which must be used and because of the difficulty of preparing nonrectifying contacts.

C. Neutron-Activation Analysis

The quantitative estimation of aluminum in diamond using neutron-activation analysis with the reaction

$$Al^{27}(n,\gamma)Al^{28} \qquad (1)$$

[5] P. J. Dean and J. C. Male, J. Phys. Chem. Solids **25**, 311 (1964).

[6] T. Evans and C. Phaal, Proc. Roy. Soc. (London) **A270**, 538 (1962).

[7] H. B. Dyer, F. A. Raal, L. du Preez, and J. H. N. Loubser, Phil. Mag. (to be published).

[8] E. C. Lightowlers, Ph.D. thesis, London, 1964 (unpublished).

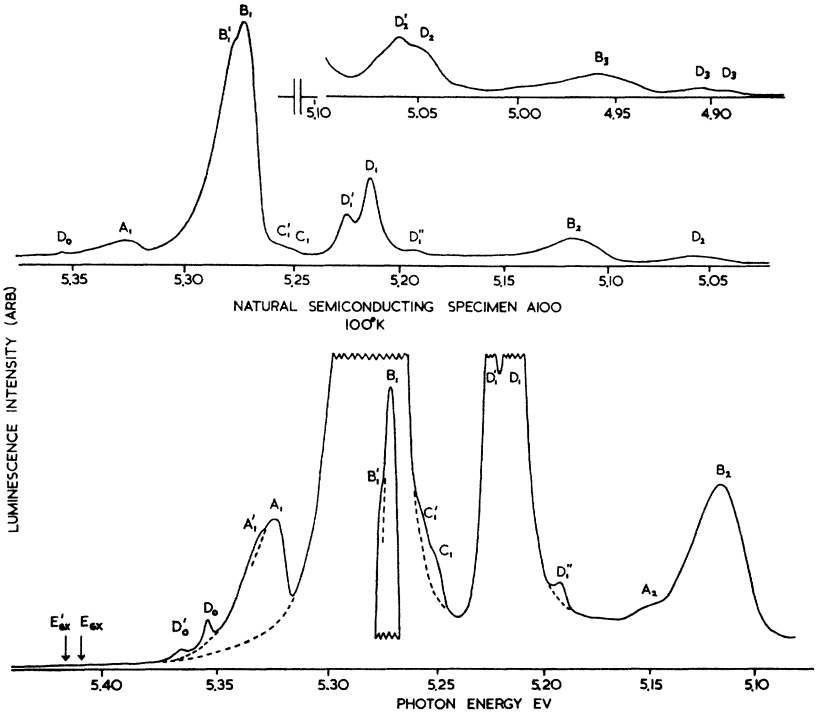

FIG. 1. Edge-recombination-radiation spectra from a relatively strain-free natural *p*-type semiconducting diamond at 100°K. The notation is discussed in the text. Resolution, 3 meV.

has already been described.[9] The main difficulty arises from the short life of the 1.78-MeV γ emission of Al^{28} (2.27 min). Using counting equipment close to the DIDO reactor, it proved possible to clean and mount the specimens in the γ-ray spectrometer in just over one half-life after 10-min irradiations at a thermal-neutron flux of $\sim 5\times 10^{12}$ n cm^{-2} sec^{-1} and a fast neutron flux of $\sim 5\times 10^{9}$ n cm^{-2} sec^{-1}. The integrated dose of fast neutrons was therefore $\sim 3\times 10^{12}$ n cm^{-2}, and was far too small to produce experimentally significant lattice damage.[10] The measurements can therefore be regarded as completely nondestructive.

The limiting practical sensitivity for Al^{27} was $\sim 2\times 10^{-9}$ g under these conditions. The shaped natural IIb specimens available for the electrical measurements weighed 20 to 30 mg, so that concentrations of $Al^{27} \gtrsim 10^{16}$ cm^{-3} could be measured. Typical concentrations are $\sim 5\times 10^{16}$ cm^{-3} (Table IV), so that the results of individual measurements were obtainable with a $\pm 20\%$ confidence level.

III. RESULTS AND DISCUSSION

The detailed edge-emission spectrum from a natural semiconducting diamond at 100°K is shown in Fig. 1. The upper and lower spectra are taken at a high recording gain and show the details of the central low-gain spectrum. The earlier component notation[2] has been amended in accordance with the new interpretational scheme discussed in Sec. III A1.

The extrinsic components *XY*, present in spectra from non-semiconducting diamond,[2] have also been closely re-examined. The previously quoted energies of these components at ~ 100°K have been found to be overestimated by ~ 5 meV. The new work has shown that the *XY* components are the emission version of the "N9 system" absorption "doublet" prominent near 5.26 eV in the edge-absorption and luminescence-excitation spectra of insulating type-I, intermediate and "type-IIa" natural diamonds.[11,12] Comparison of the emission and absorption spectra shows that *XY* are *zero-phonon* components and that the ~ 10-meV *X-Y* splitting arises in the excited state. The splitting is likely to be due to spin-orbit splitting of the hole state of a bound exciton, as discussed in Sec. III B1 for the *D* components of Fig. 1. A detailed discussion of the *XY* and other apparently associated lower energy zero-phonon components (down to ~ 4.66 eV) will be presented in a subsequent paper.

We will now discuss the typical "type-IIb" edge-emission spectrum of Fig. 1. It is convenient to examine the intrinsic components, involving the radiative recombination of free excitons, separately from the extrinsic components, which are due to the decay of excitons bound to one particular type of point defect in the crystal lattice.

[9] E. C. Lightowlers, An. Chem. **34**, 1398 (1962).
[10] C. D. Clark, P. J. Kemmey, and E. W. T. Mitchell, Discussions Faraday Soc. **31**, 96 (1961).
[11] F. A. Raal, Proc. Phys. Soc. (London) **74**, 647 (1959).
[12] P. J. Dean and J. C. Male, Proc. Roy. Soc. (London) **A277**, 330 (1964).

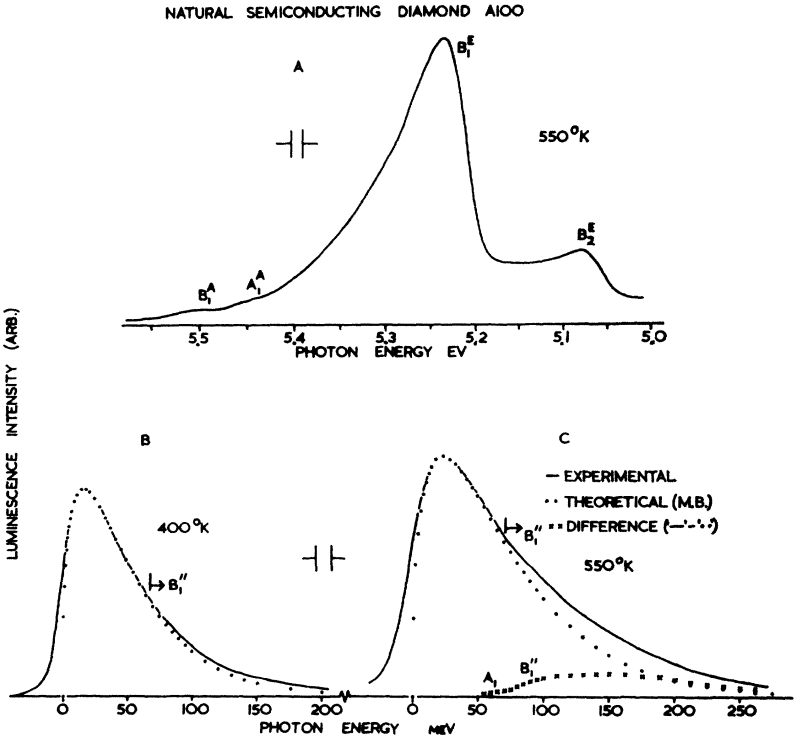

FIG. 2. Edge-recombination-radiation spectra from a natural p-type semiconducting diamond at high temperatures. A–Emission spectrum at 550°K. B–Analysis at 400°K of main intrinsic component B_1^E of the edge recombination radiation spectrum using a single Maxwell-Boltzmann (M.B.) theoretical curve. C–As B but at 550°K. Component B_1'' is due to the radiative recombination of free unbound electrons and holes (see text). Resolution, 12 meV.

A. The Single-Phonon Region of the Intrinsic Recombination-Radiation Spectrum

1. The Analysis of the Spectrum

Comparison of Fig. 1 with the emission spectra from various types of natural diamond[2] and with calculations made from the edge-absorption spectrum[13] strongly suggests that the components A, B, and C are *intrinsic*. These components represent recombinations within the perfect lattice distorted only by the presence of quanta from the normal-mode spectrum of lattice vibrations. The extrinsic components D are observed with specimen-dependent variable intensity relative to A, B, and C in spectra from IIb specimens, and are entirely absent for intermediate or type-IIa crystals. Edge emission cannot be detected from type-I diamonds under available excitation rates.

The shape of the edge absorption components[13] clearly demonstrates that the lowest energy gap between the valence and conduction band is indirect, involving a change of electron momentum ($\mathbf{K}_c - \mathbf{K}_v \neq 0$). Analysis shows that bound electron-hole (exciton) states, rather than free carrier states, are created in the near threshold phonon-assisted optical absorption transitions. The exciton binding energy E_x is 0.07 to 0.08 eV.[12,13] E_x is ~0.008 eV for silicon, and the radiative recombination rate for free electrons and holes is only $\sim\frac{1}{6}$ of the exciton recombination rate at 83°K, and is negligible at 18°K.[14] The edge-emission spectra from diamond at $\lesssim$200°K should therefore be dominated by the recombinations from exciton states. This prediction is experimentally confirmed. Only the main intrinsic components B_1 and B_2 can clearly be resolved in the spectra obtained above 300°K, and the integrated spectral intensity is much less than at 100°K. In spite of this it can be seen that at $T \gtrsim 400$°K component B_1 contains extra radiation on the high-energy tail commencing near B_1'', E_x (~80 meV) above the low-energy threshold of B_1, due to the recombination of free unbound electron-hole pairs (Fig. 2). Extra radiation is also observed at energies $\gtrsim$60 meV above the B_1 threshold, apparently due to the thermally broadened A_1 component (Fig. 1). Extra radiation is also apparent at 550°K, but not at 400°K, near to 5.5 eV (Fig. 2). Component B_1^A is clearly defined and involves the annihilation of an indirect exciton with the *absorption* of a phonon from the lattice. The very weak component A_1^A probably corresponds to component A_1 of Fig. 1 but with the absorption of the momentum conserving phonon. Components A_1^A and B_1^A are both subject to appreciable self-absorption distortion[13] even though the primary excitation only penetrates ~50μ below the crystal surface. A detailed analysis of the component shape has, therefore, only been made for component B_1^E. Component B_2^E, which

[13] C. D. Clark, P. J. Dean, and P. V. Harris, Proc. Roy. Soc. (London) **A277**, 312 (1964).

[14] J. R. Haynes, M. Lax, and W. F. Flood, in *Proceedings of the International Conference on Semiconductor Physics, 1960* (Academic Press Inc., New York, 1961), p. 423.

TABLE I. Energies and classification of recombination emission bands from diamonds at 100°K.

Intrinsic		Extrinsic	
Band and threshold energy (eV)	Classification	Band and peak energy (eV)	Classification
A_1'; 5.329	$E_{gx}'-(\hbar\omega)_{\mathrm{TA}}{}^{C}$	D_0'; 5.368	$E_{gx}'-E_{4x}'$
A_1; 5.322	$E_{gx}-(\hbar\omega)_{\mathrm{TA}}{}^{C}$	D_0; 5.356	$E_{gx}-E_{4x}$
B_1'; 5.275	$E_{gx}'-(\hbar\omega)_{\mathrm{TO}}{}^{C}$	D_1'; 5.227	$E_{gx}'-E_{4x}'-(\hbar\omega)_{\mathrm{TO}}{}^{C}$
B_1; 5.268	$E_{gx}-(\hbar\omega)_{\mathrm{TO}}{}^{C}$	D_1; 5.215	$E_{gx}-E_{4x}-(\hbar\omega)_{\mathrm{TO}}{}^{C}$
C_1'; 5.253	$E_{gx}'-(\hbar\omega)_{\mathrm{LO}}{}^{C}$	D_1''; 5.193	$E_{gx}-E_{4x}-(\hbar\omega)_{\mathrm{LO}}{}^{C}$
C_1; 5.246	$E_{gx}-(\hbar\omega)_{\mathrm{LO}}{}^{C}$		
		D_2'; 5.060	$E_{gx}'-E_{4x}'-(\hbar\omega)_{\mathrm{TO}}{}^{C}-(\hbar\omega)_{\mathrm{R}}$
A_2; 5.145	$E_{gx}-(\hbar\omega)_{\mathrm{TA}}{}^{Z}-(\hbar\omega)_{0}{}^{Z-C}$	D_2; 5.048	$E_{gx}-E_{4x}-(\hbar\omega)_{\mathrm{TO}}{}^{C}-(\hbar\omega)_{\mathrm{R}}$
B_2; 5.10	$E_{gx}-(\hbar\omega)_{\mathrm{TO}}{}^{C}-(\hbar\omega)_{\mathrm{R}}$		
		D_3'; 4.903	$E_{gx}'-E_{4x}'-(\hbar\omega)_{\mathrm{TO}}{}^{C}-2(\hbar\omega)_{\mathrm{R}}$
B_3; 4.93	$E_{gx}-(\hbar\omega)_{\mathrm{TO}}{}^{C}-2(\hbar\omega)_{\mathrm{R}}$ (approx.)	D_3; 4.890	$E_{gx}-E_{4x}-(\hbar\omega)_{\mathrm{TO}}{}^{C}-2(\hbar\omega)_{\mathrm{R}}$
		D_4'; 4.755	$E_{D3}'-\sim 0.15$ eV
$B_1{}^{E}$; 5.212 / $B_1{}^{A}$; 5.49 } 550°K	$E_{gx}{}^{\mathrm{Av}}-(\hbar\omega)_{\mathrm{TO}}{}^{C}$ / $E_{gx}{}^{\mathrm{Av}}+(\hbar\omega)_{\mathrm{TO}}{}^{C}$	E_0; 5.135[a] / E_1; 4.97[a]	E_g-E_A / $E_g-E_A-(\hbar\omega)_{\mathrm{R}}$

[a] Thresholds.

is evidently much broader than $B_1{}^{E}$, is discussed in Sec. III A3. The energy difference between $B_1{}^{A}$ and $B_1{}^{E}$ is twice the relevant phonon energy [Eq. (3) below] and is given in Table I.

The temperature dependence of the exciton energy gap may also be obtained from the data of Figs. 1 and 2. These new results give an energy gap about 5 meV larger than previously found from absorption-edge measurements for $100°\mathrm{K}\lesssim T\lesssim 600°\mathrm{K}$.[13]

The peak intensity of component B_1'' occurs at about 75 meV (i.e., $\sim 2kT$) above the low-energy threshold after subtraction of the high-energy tail of B_1. This suggests that the radiative-recombination cross section for free electrons and holes in diamond is effectively independent of the relative carrier velocity, as has also been observed in silicon.[14]

For the decay of free excitons, the shape of the emission components is given by

$$I/I_0=\alpha\exp[-(h\nu-h\nu_0{}^{E})/kT], \qquad (2)$$

where I_0 is an arbitrary normalization factor, $h\nu_0{}^{E}$ is the low-energy threshold of the emission component, k is Boltzmann's constant, and T the absolute temperature. The exponential factor assumes that the kinetic-energy distribution of the free excitons is nondegenerate. Since the lifetime of the excitons is probably $\lesssim 10^{-5}$ sec,[14] their density is $\lesssim 10^{18}$ cm^{-3} and the mean inter-exciton separation is therefore $\gtrsim 100$ Å. The electron-hole separation in the free exciton is only ~ 15 Å if the dielectric constant E is 5.7. The edge-absorption coefficient α is proportional to $(h\nu-h\nu_0{}^{A})^{1/2}$ for an allowed transition component with threshold $h\nu_0{}^{A}$. The absorption and emission transitions at low temperatures ($kT\ll\hbar\omega$) involve only the *emission* of phonons into the lattice, so that

$$h\nu_0{}^{A}=h\nu_0{}^{E}+2\hbar\omega; \qquad (3)$$

$\hbar\omega$ is the energy of a phonon which conserves momentum in the indirect electronic transition

$$\mathbf{K}_p=\mathbf{K}_c-\mathbf{K}_v, \qquad (4)$$

where $\mathbf{K}_p$ is the momentum of the phonon. We discuss only single-phonon-assisted components in this section. These are denoted by subscript 1 in Figs. 1 and 2. For diamond, like silicon and germanium, $\mathbf{K}_v=0$[15] so that $\mathbf{K}_p=\mathbf{K}_c$. Since there are four branches in the lattice vibrational spectrum along the major symmetry axes of the diamond-type lattice, up to four single-phonon intrinsic emission components, involving four different values of $\hbar\omega$, may be expected.

Equation (2) shows that components A_1, B_1, and C_1 should have Maxwell-Boltzmann (M.B.) shape for allowed transitions. Analysis of component B_1 (Fig. 3) shows that the experimental curve can be satisfactorily represented by *two* M.B. subcomponents for which $h\nu_0{}^{E}$ are 5.268 eV and 5.275 eV, at 100°K (Table I). These components are labeled B_1 and B_1' in Fig. 1, and cannot be resolved in Fig. 2, where a

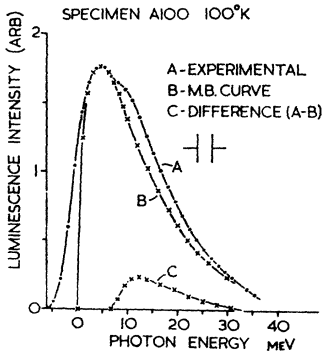

FIG. 3. Analysis of the main intrinsic component B_1 of the 100°K edge-recombination-radiation spectrum of diamond using two Maxwell-Boltzmann (M.B.) theoretical curves. Resolution 3 meV.

[15] F. Herman in *Proceedings of the International Conference on the Physics of Semiconductors, Paris, 1964* (Academic Press Inc., New York, 1965), p. 3.

single M. B. component is used in the analysis of component B_1^E. Most of the additional broadening observed on the low-energy side of the experimental curve is due to the 3-meV spectral resolution, but broadening may also arise at 100°K due to internal strain. This strain broadening appears to be exceptionally small for specimen A100 (~1.5 meV at half height at 100°K).

A study of the width of the bands in the infrared photoexcitation spectrum for holes at the acceptor center in IIb diamonds has confirmed that inhomogeneous strain broadening is exceptionally small for specimen A100. External uniaxial strains of $\lesssim 0.01\%$ cause changes in the infrared spectrum sufficient to account for the differences between the zero-stress spectra from different specimens. The components of the edge-recombination spectra of all specimens show appreciable broadening between 100 and 300°K presumably because exciton-phonon scattering becomes significant in this temperature range (Fig. 12).

Intrinsic component A_1 also contains two components, A_1 and A_1', which are clearly resolved in Fig. 1, and are similar to B_1 and B_1'. Although a quantitative test is more difficult because of the presence of the B_1, B_1' tail, it has been shown that A_1 and A_1' are also of M.B.-type shape. The thresholds of these subcomponents are given in Table I, together with those for C_1 and C_1' estimated from Fig. 1. This fine structure in the A and C components was not resolved in the earlier measurements.[2] The two B_1 subcomponents were then attributed to two different values of $\hbar\omega$ in Eq. (3). The intensity ratio of the B_1' and B_1 components decreases with decrease in temperature (Fig. 4), as is also true for the A and C subcomponents. It is, therefore, evident that these splittings have electronic origin and that thermalization occurs between the components in the excited (free exciton) state.

The magnitude of the splitting is 7±1 meV, i.e., close to the spin-orbit splitting for free carbon (~5 meV) and also to the experimental value at $\mathbf{K}_v$ determined from the thresholds of the photoexcitation spectra for the appropriate components of the cyclotron-resonance absorption spectrum of free holes in IIb natural diamonds at ~4°K (6±1 meV).[16] The splittings in Figs. 1, 3, and 4, therefore, arise from the spin-orbit splitting of the hole state of the free exciton.

Components involving excitons from the split-off valence band have not been observed in the edge-emission spectra of silicon or germanium because of the effect of the large magnitude of the spin-orbit splitting (0.05 eV for silicon, 0.28 eV for germanium) on the relevant thermal population factors. The corresponding absorption components may be observed, however.[17] For silicon carbide, the valence electrons are predominantly associated with the carbon sublattice. A splitting of 4.8 meV, observed in the extrinsic emission components due to excitons bound to neutral nitrogen donors (4D complexes–Sec. III B1), is identified with spin-orbit splitting of the hole state. The magnitude of the splitting can be influenced by the impurity potential in the bound exciton state (Sec. III B1).

The exciton energy gap, $E_{gx}=E_g-E_x$, is ~5.41 eV at 100°K.[13] The phonon energy associated with the B_1, B_1' components is, therefore, ~0.14 eV, which is half of the energy separation of components B_1^A and B_1^E in Fig. 2. This is close to the energies D_0-D_1

TABLE II. Parameters discussed and estimated from experiment.

Parameter	Energy (eV)	Description
$(\hbar\omega)_{TA}{}^C$	0.087±0.002	Transverse-acoustical phonon at $\mathbf{K}_p=\mathbf{K}_c$
$(\hbar\omega)_{TO}{}^C$	0.141±0.001	Tranverse-optical phonon at $\mathbf{K}_p=\mathbf{K}_c$
$(\hbar\omega)_{LO}{}^C$	0.163±0.001	Longitudinal-optical phonon at $\mathbf{K}_p=\mathbf{K}_c$
$(\hbar\omega)_{TA}{}^Z$	0.10 ±0.005	Transverse-acoustical phonon at $\mathbf{K}_p=\mathbf{K}_{max}\langle 100\rangle$
$(\hbar\omega)_R$	0.167±0.002	Raman phonon ($\mathbf{K}_p=0$)
E_{gx}'	5.416±0.002	Indirect exciton energy gap associated with lower valence band at 100°K (average $E_{gx}{}^{Av}$).
E_{gx}	5.409±0.002	Indirect exciton energy gap associated with upper valence bands at 100°K.
E_x	0.08 ±0.005	Binding energy of indirect exciton.
E_g	5.49 ±0.005	Indirect energy gap associated with upper valence bands at 100°K.
E_A	0.36 ±0.01	Ionization energy of aluminum acceptor center.
E_{4x}'	0.048±0.002	Binding energy of lower-valence-band indirect exciton to neutral acceptor center.
E_{4x}	0.053±0.002	Binding energy of upper-valence-band indirect exciton to neutral acceptor center.

[a] The quoted uncertainties are maximum estimated errors.

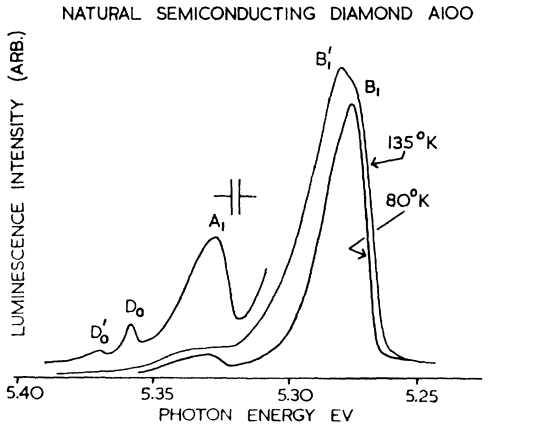

FIG. 4. Edge-recombination-radiation spectra from natural p-type semiconducting diamond showing the change in the shape of the main intrinsic component due to thermalization of the intensity of subcomponent B_1' relative to B_1. Intrinsic component A_1 is not clearly resolved at $\gtrsim$135°K. A portion of the 80°K spectrum is reproduced under high recording gain to show the narrow zero-phonon extrinsic components D_0, D_0'. Resolution 3 meV.

[16] C. J. Rauch, in *Proceedings of the International Conference on Semiconductor Physics, 1962* (Institute of Physics and the Physical Society, London, 1963), p. 276.

[17] M. V. Hobden, J. Phys. Chem. Solids. **23**, 821 (1962).

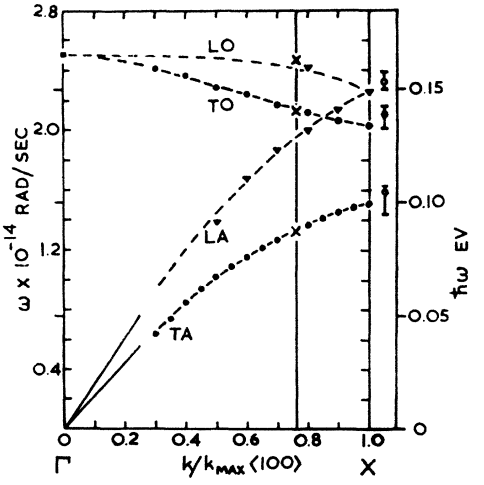

FIG. 5. The lattice-vibrational dispersion curves of diamond for ⟨100⟩-type directions determined by measurements of inelastic neutron scattering (Ref. 3). ● and ▼ are experimental points obtained from neutron scattering, ■ is derived from the Raman spectrum and points × are derived from the edge-recombination-radiation. The fit of points × to the dispersion curves locates the wave vector of the conduction-band minima (vertical line at $K/K_{max}\sim 0.76$). The analysis of the recombination-radiation spectrum supports the identification of the dispersion curves derived initially from the neutron measurements (see text).

and $D_0'-D_1'$ observed in the extrinsic spectrum (0.141 ± 0.001 eV from Table I). The D extrinsic system represents the decay of weakly bound excitons, for which the selection rule of Eq. (4) is accurately obeyed.[18,19] It is, therefore, convenient and more accurate to obtain the values of $\hbar\omega$ from the D components simply as the appropriate differences between peak energies. D_0 and D_0' are zero-phonon components (Sec. III B1). The component D_1'' is apparently the extrinsic version of C_1, so that the appropriate value of $\hbar\omega$ is 0.163 ± 0.001 eV. The weaker extrinsic component analogous to C_1' is obscured by the very strong D_1 component. The extrinsic components analogous to A_1, A_1' are masked by B_1, B_1'. The threshold values of B_1, B_1', and A_1, A_1' together with the B_1, B_1' phonon energy, give the energy of the third phonon (0.087 eV). The three phonon energies derived from Fig. 1 are therefore,

$$\begin{aligned}\hbar\omega_1&=0.087\pm0.002\text{ eV},\\ \hbar\omega_2&=0.141\pm0.001\text{ eV},\\ \hbar\omega_3&=0.163\pm0.001\text{ eV}.\end{aligned}\tag{5}$$

Two of these energies ($\hbar\omega_1$ and $\hbar\omega_2$) are similar to previously reported values.[2] The phonon $\hbar\omega_3$ was then identified with a two-phonon-assisted transition involving $\hbar\omega_2$ and a phonon of energy ~0.022 eV selected in g-type intervalley scattering between valleys on the same ⟨100⟩ axes. This explanation is not consistent with the narrow width of the D_1'' component now shown in Fig. 1. It was previously favored because $\hbar\omega_2$ should be a transverse optical (TO) phonon if the diamond and silicon emission spectra are similar as expected,[15] and it was thought that the TO phonon branch was highest in energy for all $\mathbf{K}_c\neq\mathbf{K}_0$.[20] This difficulty no longer applies (Sec. III A2).

The intensity ratio of components A_1 and B_1 is $4.8\pm0.5\%$, similar to the value reported from edge absorption,[13] and quite close to the ratio for the TA (transverse acoustical) and TO components in silicon ($\sim3.5\%$).[14] C_1/B_1 is $1\pm0.3\%$, whereas D_1''/D_1 is 1.7 $\pm0.5\%$ at 100°K. A_1'/A_1 and B_1'/B_1 are $\sim15\%$ at 100°K. At 300°K the absorption results suggest that $B_1'/B_1=60\%$,[13] but the value calculated from the emission spectra, assuming a splitting of 7 meV, is $\sim40\%$. It is likely that the absorption value is erroneous due to experimental difficulties associated with the extra breadth of the individual components at 300°K.

2. *The Position of the Conduction-Band Minima*

Assuming that $\hbar\omega_1$ and $\hbar\omega_2$ in Eq. (5) are the transverse acoustical (TA) and TO phonons (by analogy with silicon for $\mathbf{K}_c$ located along ⟨100⟩ axes) it has been shown[13] that the energies of the edge phonons cannot be reconciled with the lattice vibrational dispersion curves derived mainly from an analysis of the intrinsic two-phonon infrared absorption spectrum of diamond.[20] However, recent measurements of the complete dispersion curves for the ⟨100⟩ and ⟨111⟩ type symmetry axes from inelastic neutron scattering experiments on a 243-carat type-IIa diamond,[3] have provided a quite different set of dispersion curves (Fig. 5). $(\hbar\omega)_{LO}>(\hbar\omega)_{TO}$ in Fig. 5 for all values of $\mathbf{K}_p$ except $\mathbf{K}_p=0$, in contrast to the spectra of germanium and silicon where $(\hbar\omega)_{TO}>(\hbar\omega)_{LO}$ for most values of $\mathbf{K}_p$ (LO = longitudinal optical, LA = longitudinal acoustical). The phonon energies of Eq. (5) are in good agreement with these neutron results if $\mathbf{K}_c$ is at $(0.76\pm0.02)\mathbf{K}_{max}$ along the ⟨100⟩ type axes (Fig. 5). The LO branch derived from the neutron measurements suggests that $(\hbar\omega)_{LO}=0.160$ eV at $\mathbf{K}_c$, but the experimental point at $\mathbf{K}_p=0.8\ \mathbf{K}_{max}$ and the experimental value of $\hbar\omega_3$ [Eq. (5)] both suggest a slightly higher value. It is clear that the present results substantiate the very flat ⟨100⟩ LO branch over the inner $\frac{3}{4}$ of the reduced zone deduced from the neutron measurements.

According to Fig. 5, $(\hbar\omega)_{LA}=0.129$ eV at $\mathbf{K}_p=\mathbf{K}_c$. Thus the 100°K thresholds of intrinsic components involving the LA phonon should be at 5.280 and 5.287 eV. These components should, therefore, occur between $\sim\frac{1}{4}$ and $\sim\frac{3}{4}$ of the way up the high-energy tail of the B_1, B_1' components. No additional intrinsic components have been detected in this region, which implies that the relative intensities of the LA components are probably even lower than for the LO components C_1

[18] D. G. Thomas, M. Gershenzon, and J. J. Hopfield, Phys. Rev. 131, 2397 (1963).
[19] J. R. Haynes, Phys. Rev. Letters 4, 361 (1960).
[20] J. R. Hardy and S. D. Smith, Phil. Mag. 6, 1163 (1961).

and C_1'. It is fortunate that $(\hbar\omega)_{LO} > (\hbar\omega)_{TO}$ at $\mathbf{K}_p = \mathbf{K}_c$ in diamond, so that the weak LO components emerge below the thresholds of the intense TO components. Neither the LO nor the LA phonon-assisted components have been observed in the edge emission or absorption spectrum from silicon.

The C_1 components appear to rise less rapidly with $h\nu$ than A_1 or B_1, especially when the effects of the tails of components B_1, B_1' are allowed for (compare A_1 and C_1 in Fig. 1). This difference is difficult to assess quantitatively, but if real it may imply that the LO-phonon assisted transition is forbidden, since α in Eq. (2) is then proportional to $(h\nu - h\nu_0)^{3/2}$. This transition is not forbidden by symmetry except for transitions via the $\mathbf{K}_c = 0$ intermediate conduction band state.[21] Although this intermediate state apparently predominates for the allowed TA and TO absorption components,[13] it is perhaps surprising that allowed transitions via other possible intermediate states do not predominate for the LO components. The required degree of forbiddenness for the absent LA component has not been adequately demonstrated from group-theoretical arguments, even when time-reversal is also considered.[21]

The edge-emission spectrum of cubic silicon carbide, which is closely related to silicon and diamond in energy-band structure as well as chemically, contains extrinsic components due to the decay of 4D complexes at nitrogen donors.[22] Four single-phonon assisted components are observed corresponding to $\mathbf{K}_p = \mathbf{K}_{max}\langle 100\rangle$. These components have approximately *equal* intensities, suggesting the absence of any appreciable phonon-dependent selection rule. The conduction band is nondegenerate at X, for silicon carbide (no inversion symmetry), as are the conduction-band minima of silicon and diamond at the Δ_1 symmetry points. It is possible that these differences may be due to differences in the relative positions of the important intermediate states in the conduction and valence bands of the three crystals.

3. *The Multiphonon Region of the Intrinsic Spectrum*

One of the most striking features of the recombination spectrum in Fig. 1, is the presence and strength of the components A_2, B_2, and B_3 associated with the simultaneous emission of two or three phonons. The intensity ratios $B_2/(B_1+B_1')$ and $B_3/(B_1+B_1')$ are respectively $14\pm1\%$ and $2.4\pm0.2\%$, and the intensity ratio $A_2/(A_1+A_1')$ is similar to $B_2/(B_1+B_1')$. The multiple-phonon-assisted components are very broad. For example, the half width of B_3 is roughly twice that of B_1+B_1', and no internal structure can be resolved. This broadening is very large for component B_4, which cannot be clearly separated from the extrinsic component D_4 (Fig. 6), although components D_3 and B_3 are quite distinct. This is consistent with the possibility of a large variety in the individual wave vectors, and hence in the energies, of each of the phonons in the two- or threefold combinations. It is likely that transitions assisted by two or more phonons with *noncollinear* wave vectors, which still satisfy Eq. (4), may make a significant contribution to these intrinsic components.

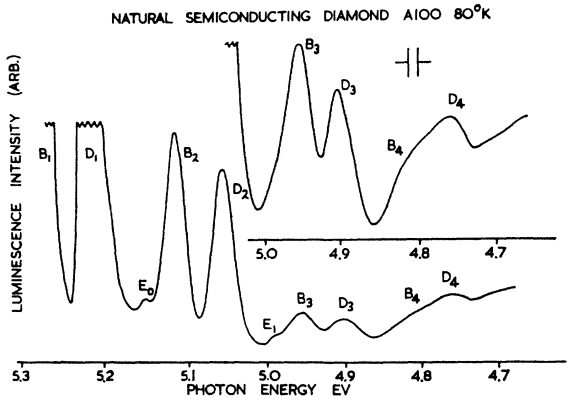

FIG. 6. Edge-recombination-radiation spectra from a natural p-type semiconducting diamond at 80°K showing the resolvable phonon-assisted intrinsic (B_1 to B_4) and extrinsic (D_1 to D_4) components. The upper spectrum was obtained using higher recording gain than that used for the lower spectrum. Resolution 12 meV.

The thresholds, $h\nu_0$, for B_2 and B_3 agree approximately with the relationship

$$h\nu_0 = E_{gx} - (\hbar\omega)_{TO} - n(\hbar\omega)_R, \qquad (6)$$

where $n = 1, 2$ and $(\hbar\omega)_R$ is the Raman energy (0.165 eV). $h\nu_0$ for A_2 is about 0.18 eV below $(h\nu_0)_A$, however, suggesting that the TA phonon is selected from near $\mathbf{K}_{max}\langle 100\rangle$ for this limiting transition. $(\hbar\omega)_{TA} \sim 0.10$ eV at the $\langle 100\rangle$ zone boundary.

As expected from these conclusions, the intensity ratios $B_2/(B_1+B_1')$ and $B_3/(B_1+B_1')$ are not consistent with the Poisson-type expression used for the corresponding D components (Sec. III B4). Assuming from $B_2/(B_1+B_1')$ that $\gamma = 0.15$, then Eq. (12) predicts that $B_3/(B_1+B_1') = 0.011$, about 50% of the observed value.

The principal intrinsic multiple-phonon-assisted recombination component from silicon also obeys Eq. (6) and contains about 8% of the single-phonon TO component intensity. Other multiple-phonon-assisted components are attributed to transitions involving intervalley scattering processes[23] and represent individually $\lesssim 3\%$ of the TO component intensity. Figure 5 shows that for diamond, the two-phonon-assisted transitions associated with the TO phonon and "g-type" intervalley scattering give $h\nu_0 = 5.18$ eV. This component would be obscured by D_1'' in Fig. 1, but there is no evidence for a suitable intrinsic component in

[21] M. Lax, in *Proceedings of the International Conference on Semiconductor Physics, 1962* (Institute of Physics and the Physical Society, London, 1963), p. 395.

[22] W. J. Choyke, D. R. Hamilton, and L. Patrick, Phys. Rev. **133**, A1163 (1964).

[23] W. P. Dumke, Phys. Rev. **118**, 938 (1960).

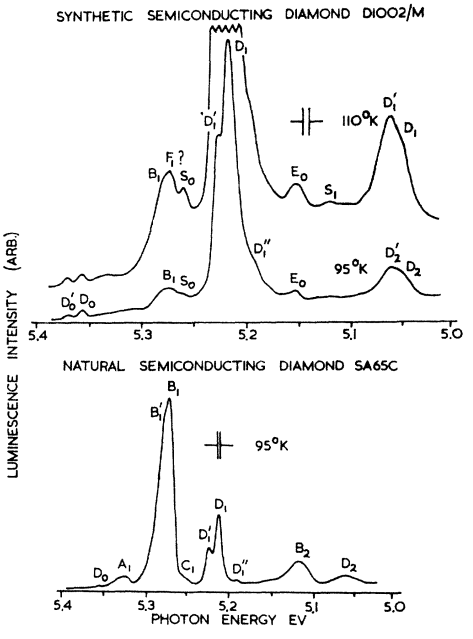

FIG. 7. Comparative edge-recombination-radiation spectra from a General Electric doped p-type semiconducting synthetic diamond (resolution, 6 meV) and from a natural South African p-type semiconducting diamond (resolution, 3 meV). These specimens were selected for the highest available concentrations of *uncompensated* acceptor centers (see text). The notation is discussed in the text. Component E_0 is attributed to the radiative recombination of electrons at neutral acceptor centers.

spectra which do not contain the D system [Fig. 2 of Ref. 2]. For scattering between valleys on different axes, $h\nu_0 \sim 5.13$ eV, and the component would be masked by B_2 (Fig. 1).

B. The Principal Extrinsic Edge Emission Components for p-type Semiconducting Diamond

The peak energies used in the previous discussion[2] of the extrinsic components shown in Fig. 1 are slightly erroneous. The interpretation will now be reviewed using the corrected energy values (Table I), which enable a mutually consistent description to be given to the intrinsic and extrinsic components.

1. Excitons Bound to Neutral Acceptors

Because the D system of components has only been observed from natural and synthetic semiconducting diamonds, which are always p-type,[24] it is natural to suggest that these sharp edge lines are due to a Lampert-type complex[25] involving excitons bound to neutral acceptor centers. This type of complex has been observed in the luminescence of a number of group IV, III–V, and II–VI crystals, and was initially recognized for silicon.[19] It has been shown that such a complex involves an electron bound to an ionized acceptor by a hole-pair bond, and the pairing of the particles within these complexes is of importance.[26] We shall describe this system as 4A since it contains 4 particles (counting the acceptor ion A).

The components D_0, D_0' are zero phonon and are quite narrow (half width ~ 2.5 meV at 75°K according to Fig. 4). They are displaced below the exciton energy gaps E_{gx} and E_{gx}' (Table 1) by 53 meV and 48 meV, which represent the binding energies E_{4x} of the excitons to the neutral acceptor. This implies that the spin-orbit splitting for the bound exciton states is 5 meV greater than for the free excitons. D_0, D_0' cannot be attributed to the decay of 3A states—i.e., excitons bound to *ionized* acceptors, since the transition energy would then be $E_g - h\nu_3$, where

$$h\nu_3 = E_A + E_3 \sim 0.13 \text{ eV} \qquad (7)$$

since $E_x \sim 0.08$ eV.

E_A is the acceptor ionization energy and E_3 is the binding energy of an electron to the neutral acceptor. The only acceptor observed in both natural and synthetic semiconducting diamond has $E_A = 0.36$ eV, i.e., nearly 5× the value necessary to satisfy Eq. (7) since the temperature dependence of the D system shows that $E_3 \sim 50$ meV.

The identification of the D system with transitions at the IIb acceptor centers is strengthened by two recent observations. Measurements of the point-by-point variations in the strength I_A of the hole photo-excitation spectrum of a polished rectangular block of type-IIb natural diamond showed that I_A was effectively zero at one end. Tests with the electron beam showed that the edge-emission spectrum failed to contain the D system *only* for the region in which $I_A = 0$. For about $\frac{3}{4}$ of the length of the block, both I_A and the intensity ratio D_1/B were effectively constant. Tests on 9 natural IIb crystals and on 20 synthetic semiconducting specimens suggest that D_1/B_1 is largest when the concentration of neutral acceptor (2A) centers is greatest. The quantitative estimation of this correlation is made difficult by the considerable inhomogeneity in most specimens, particularly the synthetics, and the very small fraction of a given specimen which can be efficiently excited by the electron beam. The ratio of the maximum concentration of 2A centers in the available General Electric synthetic specimens to that in natural strongly type-IIb diamonds was $\sim 100\times$ (Sec. III C2), and Fig. 7 shows that the D_1/B_1 ratio was also nearly 100× larger for these dark-blue synthetic crystals.

The D emission components were significantly broader in spectra from strongly doped synthetic crystals, probably due to interactions between neighboring 2A centers. The corrected half width of D for crystal D1002/M

[24] R. H. Wentorf, Jr. and H. P. Bovenkerk, J. Chem. Phys. 36, 1987 (1962).
[25] M. A. Lampert, Phys. Rev. Letters 1, 450 (1958).
[26] D. G. Thomas and J. J. Hopfield, Phys. Rev. 128, 2135 (1962).

(Fig. 7) is ~14 meV, whereas for the relatively weakly doped natural diamonds SA65C (Fig. 7) and A100 (Fig. 1) it is only ~8 meV. Broadening effects have also been observed in the infrared absorption spectra of the 2A centers in these synthetic diamonds.

Edge emission could not be detected from effectively-black doped synthetic diamonds, in which the concentration of 2A centers was presumably $>10^{19}$ cm^{-3} (Sec. III C2). Impurity banding effects should be significant within this concentration range. The integrated intensity of the edge emission was also considerably less for the deep-blue doped specimens.

The 4A complex may dissociate in either of two ways;

$$\begin{aligned} 4\mathrm{A} &\rightarrow 3\mathrm{A}+h-E_4, \\ 4\mathrm{A} &\rightarrow 2\mathrm{A}+x-E_{4x}, \end{aligned} \tag{8}$$

where x is an exciton, h a hole, and E_4 is the binding energy of the second hole. Measurements of the intensity ratio I_{D_1}/I_{B_1} between ~80°K and ~300°K were analyzed according to the expression

$$I_{D_1}/I_{B_1}=1/[1+\text{const}\,\exp(-E_{I/kT})]. \tag{9}$$

In the low-temperature region $E_I=E_{4x}=50$ meV, but at temperatures $\gtrsim$200°K, E_I was larger $\cong$70 meV. It is probable that the larger value is an artifact arising from the decrease in intensity of the whole spectrum which is especially noticeable above ~200°K. This decrease may be due to the decreasing ratio $E_{x/kT}$ and the increasing effectiveness of trapping and recombination centers for free excitons and charge carriers.

In any event these results show that $E_4\gtrsim E_{4x}$, as observed both for silicon carbide[27] and for silicon,[19] presumably because of the pairing energy of the like particles (holes). This pairing energy should be especially large if the two holes come from the same band, which may explain why E_{4x} for D_0 is ~5 meV greater than for D_0'. In the absence of thermalization, D_0' is >2× more intense than D_0 (compare D_1' and D_1 in Fig. 8 for 245°K), in contrast to the corresponding intrinsic components. The radiative decay of the 4A complex involving hole states from *different* valence bands is, therefore, >2× more probable for diamond, possibly because of the higher degeneracy of this complex. For 6*H* silicon carbide the radiative decay of the nitrogen 4D complex involving hole states from the split-off valence band is ~8× more probable than from the upper bands.[28]

The energy ratio E_{4x}/E_A is ~0.14 if $E_A=0.36$ eV. Hopfield has shown how this ratio may vary with the ratio m_e/m_h of the electron and hole effective masses in the complex.[29] It may be appropriate for this purpose to express the "chemical shift" in E_A through the

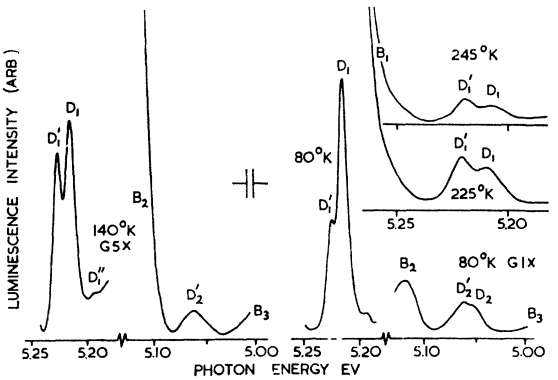

FIG. 8. Portions of the edge-recombination-radiation spectrum of a natural *p*-type semiconducting diamond (A100). The phonon-assisted extrinsic components D_1, D_1', and D_2, D_2' change shape between 80 and 140°K in accordance with the pairing D_1-D_2 and $D_1'-D_2'$ in the series of Eq. (6). These shape changes are due to thermalization. The 225 and 245°K spectra were obtained from a General Electric doped (*p*-type) semiconducting diamond (D1002/E) and show that component D_1' has the larger intensity in the absence of thermalization. Resolution 3 meV.

effective mass. When $E_{4x}/E_A=0.14$, $m_e/m_h=1.9$ and if the dielectric constant $E=5.7$, $m_h=0.87\ m_0$ for $E_A=0.36$ eV. Thus $m_e\sim 1.7m_0$, very much larger than the value ($\sim 0.2m_0$) deduced from E_x using the simple "hydrogen-like" formula.[13] The discrepancy is partially due to the use of an excessively large m_h ($\sim 3m_0$) in the calculation from E_x. Additionally, the value of E_x calculated from the free carrier values of m_e and m_h can be much greater than the observed value (20 meV, cf., 8 meV for silicon) due to the effects of the complexities of the band structure on the electron-hole correlation energy. It is, therefore, probable that a realistic value of m_e for diamond is $\gtrsim 1.0m_0$.

The intensity ratio $(D_0+D_0')/(D_1+D_1')$ is only 0.016 ±0.002. This ratio should be very sensitive to the magnitude of E_A, since E_{4A} is proportional to E_A and the electron momentum (Eq. 4) for the zero-phonon interband transition is transmitted via the exciton-impurity coupling and taken up by the recoil of the impurity ion. For exciton complexes in silicon this ratio is <0.05 for antimony ($E_D=0.043$ eV) about 1.0 for arsenic ($E_d=0.053$ eV) and about 4.0 for indium ($E_A=0.16$ eV).[30] The ratio is clearly especially sensitive to variations of E_D or E_A near to the effective mass value, and increases rapidly with increase in the chemical shift, as also observed for donors in germanium.[31] The very small magnitude of this intensity ratio for the diamond 4A complex therefore implies that the chemical shift of the 2A center is also very small. A similar conclusion is obtained from calculations of E_A on the hydrogenic approximation, although the appropriate value of m_h is somewhat uncertain and possibly specimen dependent (Sec. III C1). All that can

[27] D. R. Hamilton, W. J. Choyke, and L. Patrick, Phys. Rev. **131**, 127 (1963).
[28] W. J. Choyke and L. Patrick, Phys. Rev. **127**, 1868 (1962).
[29] J. J. Hopfield, in *Proceedings of the International Conference on Semiconductor Physics, 1964* (Dunod Cie., Paris, 1965), p. 725.
[30] J. R. Haynes (private communication).
[31] C. Benoit a la Guillaume and O. Parodi, in *Proceedings of the International Conference on Semiconductor Physics, 1960* (Czechoslovakian Academy of Sciences, Prague, 1961), p. 426.

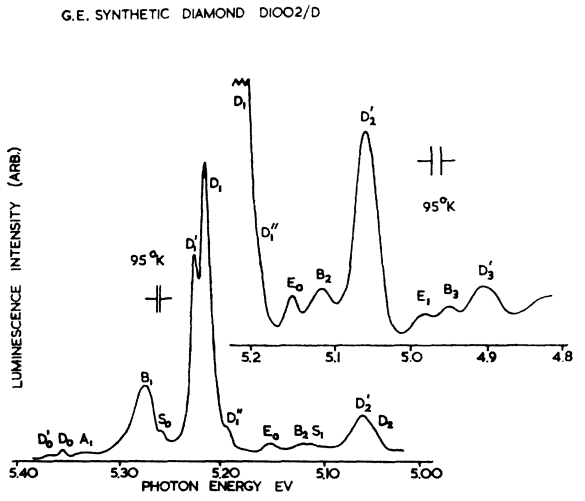

FIG. 9. The edge recombination radiation spectrum from a General Electric p-type doped semiconducting diamond at 95°K. Components E_0 and E_1 are attributed to the recombination of electrons at *neutral aluminum* acceptors. Components S_0 and S_1 may involve the radiative decay of excitons bound to *ionized boron* acceptors. Resolution 3 meV (lower spectrum) and 12 meV (upper, high gain, spectrum).

be said at present, is that the cyclotron resonance hole masses (0.7, 1.06, and 2.12 m_0)[16] and the results of *some* accurate Hall and conductivity measurements (Sec. III C1) do suggest that m_h may be $\sim 1.0\, m_0$ for some specimens, as required if $E_A = 0.36$ eV, and the appropriate value of ϵ is again ~ 5.7.

2. *Excitons Bound to Ionized Acceptors*

Hopfield has shown from consideration of the energy represented by the localization of an electron at a 2A center that excitons will not form a stable 3A complex unless $m_e/m_h \gtrsim 1.4$.[29] For $m_e/m_h \sim 1.9$, the value of E_3 in Eq. (7) is predicted to be ~ 5 meV. Judging from the behavior of the 4A complex, measurements at $T \lesssim 25$°K would be required to observed luminescence due to the decay of these 3A states. The predicted transition energy is ~ 5.12 eV. As expected, no component attributable to the decay of these 3A complexes has been observed in the present investigations, which were restricted to $T > 75$°K.

Component S_0, observed in the emission spectra from boron-doped synthetic crystals, which also contain appreciable concentrations of the acceptors responsible for the D system (Fig. 9), is probably due to the decay of excitons bound to ionized boron acceptors. This component will be discussed in a later paper.

3. *The Radiative Recombination of Free Electrons at Neutral Acceptor Centers*

As well as components S_0 (Sec. III B2), the spectra of Fig. 9 contain two components E_0 (at ~ 5.15 eV) and E_1 (at ~ 4.98 eV) in addition to those discussed above in connection with Fig. 1. Components E_0 and E_1 have previously been observed in the edge-emission spectrum of a type-IIa specimen, which contained about 10^{16} cm^{-3} of fully compensated acceptor centers [Fig. 2 of Ref. 2]. The E components are not intrinsic and do not belong to the D extrinsic system, although they are often strong for synthetic specimens when the D system is very strong. These synthetic specimens contain at equilibrium a large relative concentration of *ionized* 0.36-eV acceptor centers (Sec. III C2), in contrast to the natural IIb crystals in which the concentration of 2A centers is typically 5× that of the ionized 1A centers.

A possible radiative recombination mechanism involves the capture of free electrons by 2A centers. This process will be more favored relative to recombinations of bound 4A complexes for high values of the concentration ratio of 1A to 2A centers, since the 1A centers will act as efficient hole traps and so reduce the concentration of free holes appreciably below the free electron concentration. The low-temperature carrier capture cross section of 2D and 2A centers in germanium and silicon has been found to be determined by a radiative decay mechanism,[32] and both zero-phonon and phonon-assisted transitions are observed. These processes were first investigated by Haynes for silicon and were prominent in the 77°K spectra.[33] More recent spectra at 25°K from arsenic-doped silicon apparently shows the simultaneous presence of zero-phonon and phonon-assisted 4D and 2D+h emission components.[19]

The electrons should obey M.B. statistics in the conduction band. The low-energy threshold of the zero-phonon emission component corresponding to the recombination of electrons at 2A centers is simply

$$h\nu = E_g - E_A \tag{10}$$

and is ~ 5.13 eV for the 0.36-eV acceptor if $E_x = 0.08$ eV. The observed threshold energy of E_0 is $\sim 5.135 \pm 0.005$ eV (Table I). The integrated intensity for E_0 is slightly *greater* than for the broad E component. This is consistent with recent observations for silicon at 30°K[34] in which the intensity of the zero-phonon component for the recombination of electrons at neutral indium acceptors is $\sim 20\%$ larger than for the TO-phonon-assisted transitions, although the zero-phonon component is negligible for recombinations at gallium acceptors. The relative intensity of these components is, therefore, a very sensitive function of the energy ratio $E_A/(\hbar\omega)_{\mathrm{TO}}{}^C$. For indium in silicon and aluminum in diamond, this ratio is ~ 2.7, whereas for gallium in silicon it is only ~ 1.2.

The phonon energy given from the separation of E_0 and E_1 (Table I) is reasonably consistent with $(\hbar\omega)_{\mathrm{R}}$

[32] Y. E. Pokrovsky, in *Proceedings of the Symposium on Radiative Recombination, 1964* (Dunod Cie., Paris, 1965), p. 129.

[33] J. R. Haynes and W. C. Westphal, Phys. Rev. **101**, 1676 (1956).

[34] Y. E. Pokrovsky and K. I. Svistunova, Fiz. Tverd. Tela **5**, 1880 (1963) [English transl.: Soviet Phys.–Solid State **5**, 1373 (1964)].

rather than $(\hbar\omega)_{\mathrm{TO}}{}^{C}$. Thus, Eq. (4) is apparently not obeyed for recombinations at this relatively deeply bound center, although it is for indium in silicon.[34] The relative half widths of E_0 and E_1 (2 to $3\times kT$) are considerably less than for the corresponding silicon components at 30°K ($\sim 5kT$). Possibly 15 to 20 meV represents a natural half width for these transitions when $E_A/(\hbar\omega)_{\mathrm{TO}}{}^{C}\sim 2.7$.

4. *Multiple-Phonon-Assisted Decay of the 4A Complexes*

The components D_2, D_3 in Fig. 1 and D_4 in Fig. 6 are the extrinsic versions of the components B_2, B_3, and B_4 discussed in Sec. III A3. The peak energies of the components D_1, D_2, and D_3 (Table I) are consistent with the equation

$$h\nu=(h\nu)_{D_0,D_0'}-(\hbar\omega)_{\mathrm{TO}}{}^{C}-n(\hbar\omega)_{\mathrm{R}}. \tag{11}$$

For these bound exciton transitions, Eq. (4) is apparently completely satisfied by the TO phonon, and subsequent optical phonons are selected at $\mathbf{K}_p=0$. The shapes of D_2 and D_3 in Figs. 1 and 8 suggest that the two- and three-phonon-assisted transitions from D_0' are considerably more probable than those from D_0, although the reverse is true for D_0, D_0' and D, D_1' at $\lesssim 100$°K. The temperature dependence of the intensity ratios D_2'/D_2 and D_1'/D_1 are mutually consistent between 80°K and 140°K, however (Fig. 8), supporting the obvious pairing of the bands. This temperature dependence derives from the thermalization of D_0 and D_0'.

It is of interest to enquire whether the behavior of these phonon-assisted components is similar to that observed for the interbound state transitions of holes bound to the type-IIb acceptor center of natural diamond.[35] The intensity ratio for an n-phonon-assisted component and a zero-phonon component is theoretically given by a Poisson-type expression[36]

$$I_n/I_0=\frac{\Delta E}{\Delta E+n\hbar\omega}\frac{\gamma_1{}^{n}}{n'}, \tag{12}$$

where ΔE is the electronic transition energy and γ_1 is a hole-phonon interaction parameter. γ_1 is inversely proportional to the volume occupied by the hole wave function, and is, therefore, much larger for the compact diamond acceptor center than for acceptor centers in silicon or germanium.[36] The high-order phonon-assisted components are correspondingly very weak and are undetectable except for diamond.

According to Eq. (11), the value of n in Eq. (12) should be one *less* than those given in Figs. 1 and 6. Table III shows the observed intensity ratios and those calculated from Eq. (12) assuming that $\gamma_1=0.19$ (from the ratio of D_2/D_1) and also for $\gamma_1=0.25$, which was the value obtained from the infrared spectra.[35] The experimental results are evidently not well described by Eq. (12) for either value of γ_1. The observed ratios D_{n+1}/D_n are not proportional to γ_1/n as expected, but tend to increase with increase of n (0.18 for $n=1$; 0.21 for $n=2$ and ~ 0.4 for $n=3$). In fact, Fig. 6 shows that the n-dependencies of the D- and B-component intensities are very similar in spite of the close agreement of D_1, D_2, and D_3 with Eq. (11). Table I shows that D_4 does not fit this series, however, and the relative intensity of this component is anomalously large (Table III). The increase of broadening between components B_3, D_3 and B_4, D_4 is also anomalous (Fig. 6). It is evident that both of these phonon-assisted component series are considerably more complicated than is suggested by Eq. (11). Possibly components D_4 and B_4 of Fig. 6 are distorted by radiation due to transitions not associated with the D and B series.

TABLE III. Analysis of the multiple-phonon-assisted extrinsic components.

Intensity ratio	Observed	Calculated ($\gamma_1=0.25\pm0.01$)	Calculated ($\gamma_1=0.19\pm0.02$)
$(D_2+D_2')/(D_1+D_1')$	0.18 ±0.02	0.24 ±0.01	0.18 ±0.02
$(D_3+D_3')/(D_1+D_1')$	0.038±0.004	0.029 ±0.002	0.017 ±0.004
$(D_4+D_4')/(D_1+D_1')$	0.015±0.003	0.0024±0.0003	0.0010±0.0006

5. *Visible Emission Spectra from Natural and Synthetic Semiconducting Diamond*

The edge excited "visible" or "band-A" luminescence of both natural and synthetic diamond has been attributed to the "pair" radiative recombination of electrons bound to deep nitrogen donors ($E_D=4.0$ eV) with holes bound to the acceptor of natural IIb diamond ($E_A=0.36$ eV).[37] The emission band stretches from ~ 1.5 eV up to nearly 4.0 eV in type-I and intermediate-type natural diamond, corresponding to donor-acceptor recombinations at very diffuse pairs (~ 1.5 eV) through nearest-neighbor pairs (~ 3.0 eV) and finally at complexes containing more than one nitrogen donor center (up to ~ 4.0 eV).

The extensive complexes and nearest-neighbor simple pairs are relatively rare for all types of semiconducting diamond, so the "visible" luminescence spectrum is largely confined to quanta of energy $\lesssim 3.2$ eV (Fig. 10). The visible emission spectra of nominally undoped or nitrogen-doped General Electric synthetic diamond peaks at about 2.1 eV, when corrected for the sensitivity curve of the $S13$ photomultiplier cathode (Fig. 10), and corresponds to transitions at diffuse donor-acceptor pairs. No edge luminescence can be detected for these specimens, presumably because the excess nitrogen donors act as efficient recombination centers like the associated nitrogen platelets of type-I natural

[35] S. D. Smith and W. Taylor, Proc. Phys. Soc. (London) **79**, 1142 (1962).

[36] J. R. Hardy, Proc. Phys. Soc. (London) **78**, 1154 (1962).

[37] P. J. Dean, Phys. Rev. **139**, A588 (1965).

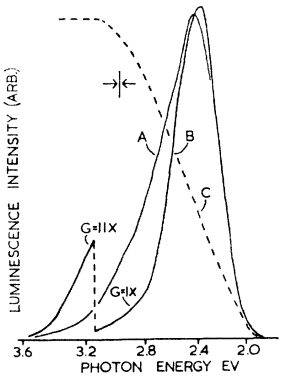

FIG. 10. *Visible* (band *A*) recombination-radiation spectra from a General Electric doped semiconducting synthetic diamond showing very weak *edge* luminescence (curve B, specimen D 1002/M) compared with that from a strongly edge-luminescent synthetic diamond (curve A, specimen D 1002/D). Curve B is also typical of the spectrum from nonedge-luminescent nitrogen-excess General Electric synthetic diamond. Curve C shows the approximate spectral sensitivity of the S13-type photomultiplier cathode used to detect the luminescence.

diamond.[38] The capture of electrons by ionized nitrogen donors is apparently nonradiative, but the recombination of holes at the neutral donors may be radiative.[37]

It has been consistently observed that the visible luminescence spectrum obtained from the doped specimens which show significant edge luminescence has a stronger high-energy tail than the spectrum from the insulating crystals (Fig. 10). This enhanced high-energy tail is often irregular and probably represents transitions at relatively associated donor-acceptor pairs which just fail to be resolved into discrete bands.[39] Because of the strong associative tendency of donors and acceptors in diamond,[37] interactions between individual donor-acceptor pairs and other donor and acceptor centers are apparently significant even in synthetic diamond. These interactions will modify the transition energy of each set of donor-acceptor pairs with given internal spacing in a variable way, and are thereby responsible for the blurring of the discrete pair emission bands. The enhanced high-energy tail in the pair spectrum suggests that the concentration of diffuse neutral nitrogen donors is relatively low, as expected for the *p*-type semiconducting specimens which show the edge luminescence.

The visible spectrum from an aluminum-doped synthetic diamond contains two peaks at about 2.3 and 2.8 eV (Fig. 11). The intensity ratio of the 2.8- and 2.3-eV peaks increases with increase in the excitation density (electron beam current at constant accelerating voltage) as expected since the transitions at very close pairs (2.8 eV) have a short decay time compared with transitions at relatively diffuse pairs (2.3 eV),[37] and are therefore more difficult to saturate.

[38] F. C. Champion, Proc. Phys. Soc. (London) **B65**, 465 (1952).
[39] D. G. Thomas, M. Gershenzon, and F. A. Trumbore, Phys. Rev. **133**, A269 (1964).

The significant feature of Fig. 11 is the appearance of the 2.3-eV component under electron beam excitation. This component is absent in the corresponding spectra from *natural* type-IIb diamonds and can only be detected under the much lower carrier excitation densities ($\sim 10^{15}$ cm^{-3} sec^{-1}) produced by a beam of 45-keV x rays.[37] This suggests that the concentration of relatively diffuse donor-acceptor pairs in the synthetic crystal is very much greater than for the natural IIb crystals, which implies that relatively few of the acceptors centers will be neutral in the unexcited crystal. This conclusion is supported by the results discussed in Sec. III C2, which suggest that the concentration of compensated acceptor centers available as partners in diffuse donor-acceptor pairs in this specimen may be nearly $10^4\times$ larger than for a typical natural type-IIb diamond.

The radiation responsible for the relatively sharp emission line at 2.14 eV, together with associated phonon-assisted components at lower energies, was observed visually to originate mainly within a well-defined plane running through the specimen. Examination under the optical microscope showed that this plane contains a large number of dark inclusions, and is probably a ⟨111⟩ twin boundary (Sec. III C2).

C. The Nature of the Common Acceptor Center in Semiconducting Diamond

We have described in Sec. III B the detailed properties of some extrinsic recombination components which are characteristic of edge luminescence for all the type-IIb natural diamonds so far examined, and also for many General Electric semiconducting synthetic crystals. These components have been identified with the recombination of excitons bound to the neutral acceptor center which is a characteristic feature of this type of crystal. The results of experiments designed to establish the chemical nature of this acceptor center will now be discussed.

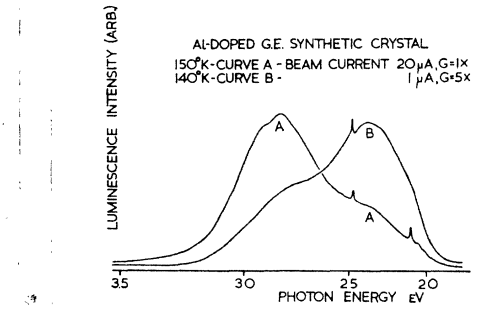

FIG. 11. Visible (band A) recombination radiation spectra from an aluminum-doped General Electric *p*-type semiconducting synthetic diamond. The relative intensity of the high energy (2.8 eV) broad component increases relative to that of the low energy (2.3 eV) component as the excitation intensity is increased. The sharp peak near 2.1 eV and the lower energy phonon-assisted components represent luminescence which originates in a well-defined plane running through the specimen, and constitute a well-known luminescence system in natural diamond.

1. Quantitative Correlation between the Acceptor and Aluminum Concentrations in Natural Semiconducting Diamond

Electrical[40] and optical-absorption[35] measurements on p-type natural semiconducting diamond are consistent with the view that these properties are dominated by the effects of one definite invariant type of acceptor center of activation energy $\sim$0.36 eV. Thermoluminescence measurements suggest the presence of a weak component with activation energy $\sim$0.21 eV.[41] Studies of the edge-excited luminescence of natural IIb crystals[37] suggest that the 0.21-eV center can be identified with the fraction of the 0.36-eV acceptor concentration whose properties are modified by the presence of *close*-neighboring ionized donor centers (Sec. III B4) and which are observed as *compensated* (permanently ionized) acceptors in the electrical measurements. If the acceptor center is due to an impurity atom which can be identified and estimated chemically, it should therefore be possible to establish a quantitative correlation between the impurity concentration and the total concentration of acceptor centers (neutral+ionized) estimated from Hall effect measurements. Qualitative studies using slow neutron activation analysis, suggested that aluminum was a plausible candidate. Quantitative tests of the possible correlation were therefore made using the experimental techniques described in Secs. II B and II C.

Only three specimens were available for the initial investigation. The results of the electrical transport measurements on specimen A100, which was the specimen used in the earlier measurements of Austin and Wolfe[42] are shown in Fig. 12. This specimen was known to have relatively homogeneous electrical and 2A-state optical properties. The temperature dependence of the hole Hall mobility μ_H was found to be smoother than previously reported, but the magnitude at 290°K (1550 ± 150 cm^2 V^{-1} sec^{-1}) is consistent with the earlier measurement. Near 290°K the mobility obeys a $T^{-1.5}$ law probably determined by acoustical phonon scattering. Above $\sim$400°K the variation is proportional to T^{-3} apparently because of the dominant effect of optical-mode carrier scattering in this temperature range.

The magnitudes of the acceptor and donor concentrations, N_A and N_D, were obtained from the temperature dependence of the free-hole concentration P using a graphical method.[43] The results were checked using a trial-and-error substitution method in the equation for the temperature dependence of P for a partially compensated semiconductor.

$$P(P+N_D)/(N_A-N_D-P)=[2\pi m_h kT/h^2]^{3/2}\times\exp(-E_A/kT). \quad (13)$$

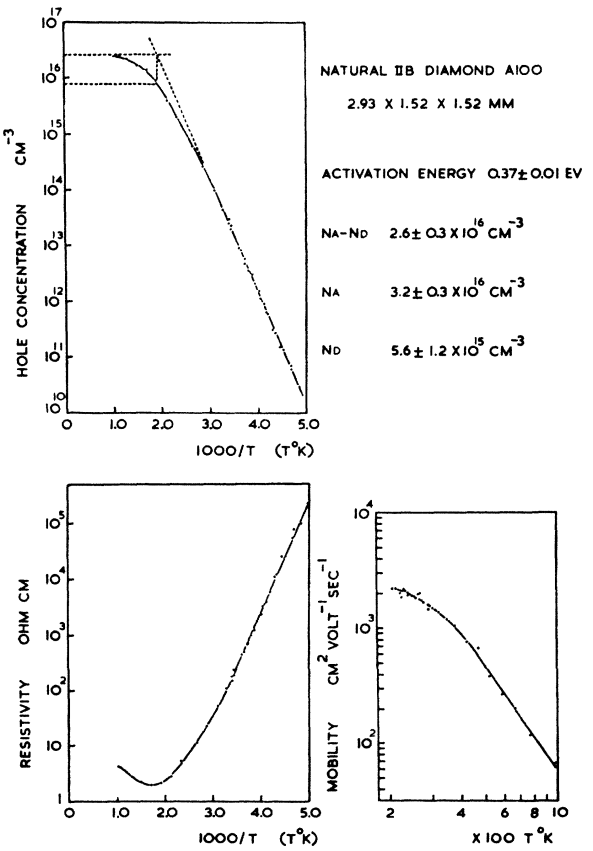

FIG. 12. Electrical transport measurements on a natural IIb diamond A100; log hole concentration and log resistivity versus reciprocal temperature, log mobilities versus log temperature. The dashed lines on the hole concentration graph are used in the graphical analysis for N_A and N_D, see Ref. 45.

For the substitution method, the value of N_A-N_D was estimated from an extrapolation of the high-temperature region of the curves of $\ln(P)$ versus T^{-1}. E_A was obtained from a plot of $k(\ln P-\frac{3}{2}\ln T)$ versus T^{-1} in the low temperature range. Values of m_h increasing by $0.1m_0$ between $0.1m_0$ and $2.0m_0$ were then substituted into Eq. (13) and the equation was solved by computer for a temperature-independent value of N_D. The results of the two methods of analysis showed good agreement. No significant variation of m_h with temperature was obtained, but the accuracy in this parameter was not high ($\pm20\%$).

The errors in the final values of N_A and N_D have both theoretical and experimental origins. The maximum error in each experimental value of the Hall coefficient R_H and resistivity ρ was $\pm5\%$. The values of P were determined from R_H according to

$$R_H=(3\pi/8)(1/Pe). \quad (14)$$

The Hall factor $3\pi/8$ is justified for nondegenerate carriers in a single spherical band for which scattering by long-wavelength acoustical phonons is predominant.

[40] P. T. Wedepohl, Proc. Phys. Soc. (London) **B70**, 177 (1957).
[41] A. Halperin and J. Nahum, J. Phys. Chem. Solids **18**, 297 (1961).
[42] I. G. Austin and R. Wolfe, Proc. Phys. Soc. (London) **B69**, 329 (1956).

TABLE IV. Results of Hall-effect and electrical-conductivity measurements.

Specimen	E_A eV	$N_A \times 10^{16}$ cm^{-3}	$N_D \times 10^{16}$ cm^{-3}	μ_h (290°K) cm^2 V^{-1} sec^{-1}	m_h/m_0
A100	0.369±0.007	3.2±0.3	0.56±0.12	1550±150	1.1±0.2
E3	0.365±0.007	7.1±0.7	0.3 ±0.06	1550±150	1.1±0.2
E4	0.374±0.007	3.3±0.3	0.11±0.02	800±80	0.4±0.1
A100 (Austin and Wolfe)	0.38	2.2	0.2	1550±150	1.0 (assumed)

The valence-band maximum in diamond is effectively triply degenerate for electrical measurements at $T \gtrsim 100$°K, and Fig. 12 shows that the dominant scattering mode is temperature-sensitive. An accurate estimate of the appropriate temperature-dependent Hall factor in Eq. (14) must await more detailed experimental work, for example, on the temperature dependence of the ratio of the Hall and drift hole mobilities. Since the variation of this mobility ratio with magnetic-field strength is similar for diamond[44,45] and silicon,[46] we are probably justified, at present, in the assumption that the departure of the Hall factor from $3\pi/8$ does not exceed 30% at any temperature.

The results of the electrical measurements are listed in Table IV. The quoted accuracies of N_A and N_D do not include the effects of possible deviations from Eqs. (13) and (14), but the graphical method used to find N_A and N_D does not depend on the right-hand-side of Eq. (13) in which theoretical uncertainties may occur.[47]

Specimen E4, which exhibits low values of μ_h and m_h and a less smooth variation of μ_H with T than shown in Fig. 12, was known to possess severe macroscopic internal strain inhomogeneities.[48] It is now believed that the associated luminescence and birefringence inhomogeneities in this diamond are due to the presence of a ⟨111⟩ twin boundary running diagonally through the block. The values of E_A, μ_H, and m_h for specimens A100 and E3, which do not show this type of large-scale strain inhomogeneity, are mutually consistent.

The hole masses for A100 and E3 are considerably larger than those obtained in earlier measurements [$(0.4\pm0.2)m_0$[40]] and appear to be more consistent with the 4°K cyclotron resonance masses for the three valence bands (Sec. III B1). It has been claimed that a value as low as $0.5m_0$ may be obtained theoretically,[49] using the 4°K band parameters and assuming that the relaxation time for carriers in the light mass band ($m^*=0.70m_0$ at 4°K) greatly exceeds the values for the other two bands at the temperatures of Fig. 12. These scattering times are approximately constant when impurity-scattering predominates for example, at 4°K.[16] The effective-mass estimates of Table IV were obtained at temperatures appropriate for *lattice* scattering, however (Fig. 12).

The results of Table IV are in good agreement with recent independent accurate measurements on three other type-IIb diamonds,[50] although a slightly lower value of E_A (0.35 eV) was found. These authors also used Lee's method of analysis[43] of the Hall data, with a Hall factor of $3\pi/8$. It is suggested that the low values of the effective mass obtained by previous workers[40] might be due to the use of a low value of the acceptor-state degeneracy parameter. In the present work this parameter was assumed to be 2 [in the right-hand denominator of Eq. (13)] in agreement with Wedepohl,[40] so that this possibility cannot explain the larger values of m_h in Table IV. The present authors feel that low values of m_h may arise from the presence of twin planes as discussed above for specimen E4, and possibly other types of large-scale crystal defects which can disturb the Hall-effect distribution within the sample and also affect the carrier scattering process. Low-order polysynthetic twinning on ⟨111⟩ planes apparently *usually* produces disturbances in magnetoresistance measurements on IIb diamonds[50] of magnitude sufficient to obscure any effects due to the possible anisotropies in the structure of the valence bands of the perfect diamond lattice.

The values of N_A taken from Table IV and converted to the equivalent weights of aluminum in the blocks agree quite well with the weights measured by neutron activation analysis (Table V) for specimens A100 and E4, but the calculated value is significantly *larger* than the directly measured quantity for E3.

Electrical tests on E3 had suggested that the acceptor centers were not uniformly distributed as assumed in Table IV, but were concentrated in a layer adjacent to the large face of the rectangular parallelepiped around which the electrical contacts were established. Measurements of the intensity of the inte-

[43] P. A. Lee, Brit. J. Appl. Phys. **8**, 340 (1957).
[44] A. C. Beer, J. Phys. Chem. Solids **8**, 507 (1959).
[45] R. T. Bate and R. K. Willardson, Proc. Phys. Soc. (London) **74**, 363 (1959).
[46] A. C. Beer, Solid State Phys. Suppl. **4** (1963).
[47] E. H. Putley, Proc. Phys. Soc. (London) **72**, 917 (1958).
[48] P. J. Dean and J. C. Male, Brit. J. Appl. Phys. **15**, 101 (1964).
[49] P. E. Clegg and E. W. J. Mitchell, Proc. Phys. Soc. (London) **84**, 31 (1964).
[50] G. R. Leef, D. C. Seeley, and H. G. Nordlin, final report of work performed at the International Telephone and Telegraph Laboratories under U. S. Air Force Contract No. AF 19(628)-225, 1964 (unpublished).

grated infrared absorption of the blocks supported this view. At 80°K the integrated absorption of the acceptor photoexcitation spectrum is proportional to N_A-N_D, since P can be neglected (Fig. 12). The intensity ratios of the acceptor absorption band at 0.347 eV were 1.44 (E3/A100) and 1.04 (E4/A100), whereas the corresponding ratios of $(N_A-N_D)_{\text{electrical}}$ were 2.6 and 1.2.

The results of Table V can therefore be advanced as reasonable proof that the acceptor centers are due to aluminum impurities which are mainly in dispersed subsitutional lattice sites, and not clustered together. This is consistent with x-ray topographs of natural IIb diamond, which show that although high concentrations of dislocations are present, the dislocations are apparently undecorated.[51]

These measurements are, at present, being extended to other specimens using improved techniques of electrical measurements. The crystals are being surveyed optically, and only those which exhibit relatively homogeneous values of (N_A-N_D) and freedom from the effects described in Ref. (48) will be used in the later correlation tests. It is also hoped to obtain more accurate data on m_h and μ_H and their temperature variations.

2. *Qualitative Evidence from Some General Electric Doped Synthetic Diamonds*

Detailed optical-absorption and edge-luminescence studies have been made on one aluminum-doped and a selection of about 20 nominally boron-doped General Electric synthetic diamonds. The infrared optical-absorption measurements will be discussed in detail in a subsequent paper. Neutron activation analysis showed that *all* of these specimens contain between 1 and 2 $\times 10^{19}$ cm^{-3} aluminum atoms. The aluminum concentration is independent of the color of the visible light transmitted by the boron-doped specimens, which were tested in three color-sorted batches (2 mg, pale yellow; 5 mg, pale blue; 30 mg, dark blue).

The relatively large ($\sim 350\,\mu$g) aluminum-doped specimen showed the steel-blue color characteristic of natural IIb diamond. Neutron analysis showed that (apart from aluminum and nitrogen) this synthetic diamond possessed the good chemical purity also found for natural IIb crystals. The 295°K conductivity, the strength of the infrared absorption spectrum, and the ratio of the D and B components in the edge luminescence spectrum were all consistent with a value of N_A-N_D *similar* to that found in natural diamond ($\sim 5\times 10^{16}$ cm^{-3}). Thus if most of the aluminum atoms occupy substitutional sites without appreciable clustering, more than 99% of the available acceptor centers must be compensated by deep nitrogen donors. This particular crystal is twinned and has shown exceptionally strong anomalous x-ray diffraction spikes[52] which suggest the presence of associated defect structures on ⟨111⟩ planes, unlike the associated nitrogen ⟨100⟩ platelets characteristic of type-I diamond.[6] These defects may or may not be due to the aluminum. The visible emission from the aluminum doped synthetic crystal was *not* as intense as would be expected if the electrically inactive aluminum was *all* present in unassociated substitutional sites and compensated by nitrogen donors.

TABLE V. Correlation test of IIb acceptor concentration with aluminum content.

Specimen	$N_A\times 10^{16}$ cm^{-3} (Electrical)	Equivalent Al $\times 10^{-9}$ g (Electrical)	Experimental Al $\times 10^{-9}$ g (Activation analysis)
A100	3.2±0.3	9.8±0.9	11.7±2.1 11.4±2.0
E3	7.1±0.7	8.1±0.8	12.7±2.3 2.6±0.9 2.8±0.9
E4	3.3±0.3	7.0±0.7	9.3±1.7 11.0±2.0

The infrared absorption measurements on the "boron-doped" diamonds show that the nearly water-white crystals contain values of (N_A-N_D) for the aluminum acceptor between 1 and 10× those of natural IIb diamonds. The same ratio for the pale-blue specimens is ~ 20 to 30, and is $\gtrsim 100$ in the dark-blue synthetic diamonds. These crystals were ~ 0.1 to 0.2 mm thick. Some of the specimens were completely opaque in the visible and infrared (up to at least 15 μ) and no edge luminescence could be detected. The edge luminescence of the dark-blue specimens was very weak, but it could be seen that the intensity ratio of the D and B components was nearly 100× that observed for the natural IIb crystals under the same conditions (Fig. 7). The exceptionally intense *green* luminescence exhibited by the blue crystals, characteristic of transitions at diffuse donor-acceptor pairs (Sec. III B4), suggests that the variation of N_A-N_D among the crystals may be mainly due to variations of N_D, and that the majority of the essentially specimen-independent aluminum concentration is incorporated in the substitutional unassociated form.

The view that the dominant acceptor center in these synthetic diamonds is the same as in natural IIb crystals is also supported by four-terminal electrical conductivity measurements made on the aluminum-doped specimen between 220 and 320°K, which gave $E_A=0.35\pm 0.01$ eV. This result is consistent with the values in Sec. III C1, and with the value previously reported for aluminum-doped synthetic diamond.[24] The absorption bands at 0.305, 0.348, 0.364, 0.462, and

[51] E. R. Czerlinsky, A. D. Johnson, and G. H. Schwuttke, in *Proceedings of the International Conference on Diamonds in Industry, 1962* (Industrial Distributors, London, 1962), p. 265.

[52] H. O. A. Meyer and H. J. Milledge, Nature, **199**, 167 (1963).

0.508 eV, which are characteristic of the photoexcitation spectra of natural IIb diamonds, have been resolved in the infrared spectra of these aluminum and boron-doped synthetic diamonds.

No evidence has been found of a photoexcitation spectrum attributable to boron, so that any incorporated boron acceptors must be completely ionized as suggested by the edge-luminescence spectra (Sec. III B2). It is to be expected that the boron acceptors ($E_A \sim 0.2$ V)[24] will be fully ionized in crystals which also contain a high concentration of predominantly ionized aluminum acceptors ($E_A = 0.36$ eV).

IV. CONCLUSIONS

The intrinsic components of the edge-emission spectra of diamond are due to the annihilation of indirect excitons involving hole states from each of the two maxima in the valence band. Components involving the emission of three of the four possible phonons have been resolved. The energies of two of these phonons can be obtained with greater accuracy from extrinsic emission components which are due to the decay of excitons bound to neutral acceptor centers. The phonon energies are consistent with the new lattice-vibrational dispersion curves of diamond, so that the position of the conduction-band minima has now been accurately located.

Only those extrinsic components attributable to transitions involving the well-known acceptor center of natural semiconducting diamond have been considered in detail. Emission components involving the zero-phonon and phonon-assisted decay of excitons bound to this (neutral) acceptor center and also the capture of free electrons by the neutral center have been analyzed in detail. The extrinsic components yield information which is consistent with that obtained from the intrinsic components and with the behavior of similar complexes in silicon.

Comparison of the edge-emission spectra, infrared absorption spectra, the electrical transport properties, and radiochemical analyses of natural and some General Electric semiconducting diamonds has shown that this acceptor center is due to isolated substitutional aluminum atoms. The concentration of neutral aluminum acceptors may be much higher ($>100\times$) in synthetic diamond than has ever been observed in natural diamond. There is a tendency towards heavy compensation, especially for the synthetic specimens. The visible luminescence spectra suggest that much of the compensation is due to deeply bound donor centers, which are thought to be due to nonassociated substitutional nitrogen.

ACKNOWLEDGMENTS

The authors are grateful to Dr. F. A. Raal of the Diamond Research Laboratory, Johannesburg, and to W. F. Cotty of Industrial Distributors, London, for the provision of natural semiconducting diamonds. The boron-doped synthetic diamonds were obtained through the good offices of Dr. P. Cannon, of the General Electric Company, Schenectady. The aluminum-doped synthetic specimen was kindly loaned by Dr. H. O. A. Meyer of University College, London, and was initially provided by Dr. R. H. Wentorf of the General Electric Company, Schenectady. Thanks are also due to Dr. W. F. Sherman for advice and interest, particularly concerning the infrared spectral measurements, and to A. J. Collins for taking many of the infrared spectra. Dr. J. L. Warren kindly made available, before publication, the phonon dispersion curves shown in Fig. 5.

One of us (D. R. W.) is grateful to the D. S. I. R. for the provision of a maintenance grant.